UAV-Aided Multi-antenna Relay Systems with Wireless Power Transfer for Maritime Communications

Yuheng Li[1,2,3], Zhiquan Zhou[1,2,3], Jinlong Wang[1,2,3(✉)], Lina Wang[1,2,3], and Chenxu Wang[1,2,3]

[1] School of Information Science and Engineering, Harbin Institute of Technology, Weihai 264209, China
[2] Shandong Provincial Key Laboratory of Marine Electronic Information and Intelligent Unmanned Systems, Weihai 264209, China
[3] Key Laboratory of Cross-Domain Synergy and Comprehensive Support for Unmanned Marine Systems, Ministry of Industry and Information Technology, Weihai 264209, China
jlw@hit.edu.cn

Abstract. With the increase in maritime activities, traditional communication methods can no longer meet the needs of today's maritime work, and the use of unmanned aerial vehicle(UAV) relay communications in marine scenarios has attracted more and more attention. In this paper, A long-distance three-node two-hop UAV relay system for maritime users is investigated. The UAV aerial relay node first transmits an energy-carrying radio frequency (RF) signal to the maritime user node, which then harvests energy and sends data information back to the UAV aerial relay node, which in turn forwards it to the land node. Considering the peculiarities of maritime communication channels, a novel land-air-maritime communication channel model is proposed. Utilizing Zero-Forcing/Zero-Transmission (ZFR/ZFT) technology, a precoding matrix for the aerial relay node is designed, followed by simulation and emulation, the performance of the channel is tested in the case of different transmission power of relay nodes or different number of antennas of relay nodes.

Keywords: Maritime wireless communication · UAVs aerial relay · Wireless power transfer · MIMO communication

1 Introduction

With the rapid development of the United Nations' global marine science initiative, "United Nations Decade of Ocean Science for Sustainable Development",

This work was supported in part by the National Natural Science Foundation of China under Grant U23A20336, and in part by the Major Scientific and Technological Innovation Project of Shandong Province of China under Grant 2022ZLGX04, Grant 2021ZLGX05, and Grant 2020CXGC010705.

H.-H. Chen and W. Meng (Eds.): WiSATS 2024, LNICST 606, pp. 174–185, 2025.
https://doi.org/10.1007/978-3-031-86203-8_15

there is an increasing emphasis on activities related to marine climate, observation, and security. Compared to land, the vast and open expanse of the ocean means that various activities based on the ocean are highly dispersed, making it difficult to establish connections between them. For example, despite maritime transport being the main tool for global trade, communication methods still rely on radio or satellite phones. During sea voyages, crew members cannot access real-time, rich multimedia entertainment services. Additionally, the communication channels in the maritime environment differ significantly from those on land. For instance, land communication is often obstructed by tall buildings, making it difficult to establish direct links, whereas in the maritime environment, the absence of obstacles allows direct links to account for the majority of communication. Furthermore, the motion of maritime users, caused by the constant movement of water, greatly complicates the establishment of communication links.

Currently, maritime wireless communication mainly uses medium/high-frequency communication and very high frequency (VHF) communication via satellites as "bridges" to interact with land. Unfortunately, the implementation costs of these methods are extremely high, and due to bandwidth limitations, they cannot achieve high-speed multimedia services. The primary research approach in current marine communication is to apply mature technologies from terrestrial communication networks, such as worldwide interoperability for microwave access(WiMAX), long term evolution(LTE), and wireless local area network(WLAN) to marine scenarios for designing marine communication systems [1–8].

On the other hand, with the rapid development of unmanned aerial vehicles (UAVs), more and more long-endurance, high-load UAV equipment has emerged, bringing infinite possibilities for their application in marine communication. LTE, WiMAX, and other communication systems can extend communication distances in marine scenarios using UAVs as relays [8]. In [2], Kim et al. networked the maritime broadband communication (MariComm) bridge as a maritime heterogeneous relay network, achieving at least 1 Mbps broadband internet/multimedia service at sea. In [9], Qi et al. studied the throughput issues of the maritime Internet of Things (MioT) and proposed using UAVs as aerial relays to improve system throughput. [10] proposed a cooperative multicast communication scheme based on joint beamforming (BF) optimization and relay design to support multimedia services for maritime users. In [11], Li et al. proposed a multi-UAVs relay maritime wireless communication network (MWCN) system model for network services, achieving dynamic trajectory and optimal flight attitude adjustments of UAVs through a dual Q-learning-based UAV trajectory adjustment algorithm (UTAA-DQ). In [12], Ji et al. proposed a cooperative relay network (CRN) scheme combining partial decode-and-forward (P-DF) and non-orthogonal multiple access (NOMA) for maritime spatial communication. This scheme forwards successfully decoded symbols from coastal base stations to ship users via island relay nodes to avoid performance loss caused by high decoding requirements in full decode-and-forward (DF) schemes.

Moreover, wireless power transfer (WPT) technology can provide energy transfer to distant electronic devices without physical connections, allowing wireless communication devices to start and operate in scenarios without fixed power supplies. Thus, this technology has gained favor from academia and industry [13,14]. Previously, limited by antenna materials and communication technology, traditional radio frequency (RF) signals could only be used for either information transmission or energy transfer. However, with the advancement of antenna materials and communication technology, it has become possible to use antenna modules for both information and energy transfer. WPT technology is gradually helping to solve the energy supply problems of wireless devices in long-distance scenarios such as in the air, far sea, and underwater. Based on principles, WPT technology is divided into electromagnetic induction mode, electromagnetic resonance mode, and electromagnetic radiation mode. He et al. in [15] proposed a wireless power and information dual transmission (WPIDT) system that uses the frequency mixing characteristics of inverters/rectifiers to modulate information signals onto the sidebands of the power carrier and transmit them through mid-range channels. In [16], Li et al. proposed a sub-wavelength WPT framework combined with deep learning-driven environmental sensors to achieve intelligent wireless energy transmission to multiple targets in dynamic environments. In [17], Wang et al. designed a UAVs-assisted NOMA network model, using UAVs to transmit energy and information to ground passive receivers (PRs).

2 System Model

We designed a three-node two-hop MIMO communication system, where maritime user node U transmits information to land source node S via an aerial relay node R, as shown in Figure. 1. The maritime user node, aerial relay node, and land source node are equipped with N_U, N_R, and N_S antennas, respectively. We assume that the aerial relay node and land source node have their power supplies, while the maritime user node needs to collect RF energy sent from the aerial relay node for power. Specifically, a communication cycle is divided into three stages. First, the aerial relay node transmits energy-carrying signals to the maritime user node to activate it. Then, the maritime user node converts data collected by its sensors into information signals and transmits them to the aerial relay node. Finally, the aerial relay node linearly precodes the received information signals and transmits them to the land source node. Unlike other relay communication systems, we considered the characteristics of maritime user nodes like ocean buoys without fixed power supplies, providing energy through aerial relay nodes' wireless charging, making it more suitable for maritime wireless communication environments.

We adopted a time-switching mode for energy and information transmission. In this mode, the total time of a communication cycle is divided into three parts, represented by the time-switching coefficient $\alpha\,(0 < \alpha < 1)$. In the first time period, the aerial relay node transmits energy to the maritime user node for duration αT. In the second time period, the maritime user node transmits

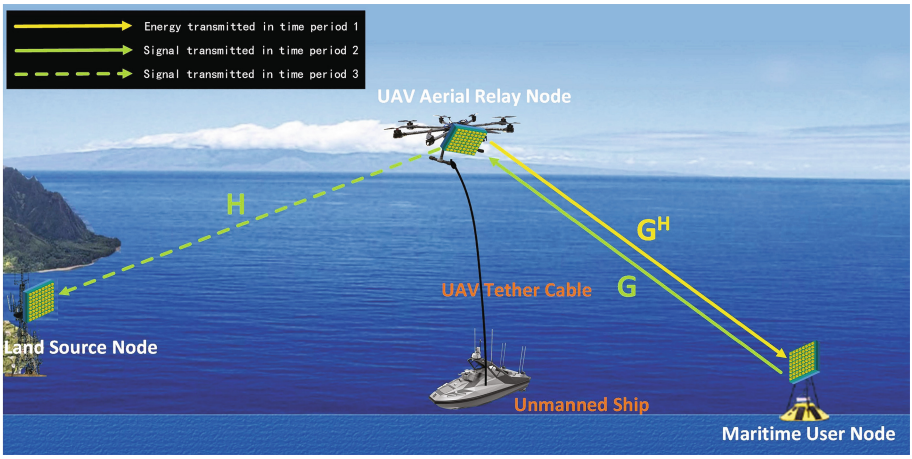

Fig. 1. A three-node two-hop MIMO relay communication system with an energy harvesting relay node.

signals to the aerial relay node for duration $(1-\alpha)\,T/2$. In the third time period, the aerial relay node forwards the signals to the land source node for the same duration $(1-\alpha)\,T/2$.

In the first time period, the aerial relay node adopts an average power allocation method, pre-coding the $N_R \times 1$ energy-carrying signal vector $\mathbf{s}_i$ with matrix $\mathbf{F}_R = \sqrt{P_R/N_R}\mathbf{I}_{N_R}$ and transmitting it to the maritime user node, where $\mathbb{E}\{\mathbf{s}_i\mathbf{s}_i{}^H\} = \mathbf{I}_{N_R}$, P_R is the transmit power of the relay node, $\mathbb{E}\{\cdot\}$ representing the statistical expectation, $(\cdot)^H$ denoting the Hermitian transpose, and $\mathbf{I}_{N_R}$ being $N_R \times N_R$ the identity matrix. The received energy signal vector at the maritime user node can be expressed as

$$\mathbf{y}_D = \sum_{i=1}^{N_R} \mathbf{G}^H \mathbf{F}_R \mathbf{s}_i + \mathbf{n}_U\,, \tag{1}$$

where $\mathbf{G} \in \mathbb{C}^{N_R \times N_U}$ is the MIMO channel matrix between the maritime user node and the aerial relay node, $\mathbf{n}_U$ is the zero-mean additive white Gaussian noise (AWGN) at the maritime user node with $\mathbf{n}_U \sim \mathcal{CN}(\mathbf{0}, \sigma_{N_U}^2 \mathbf{I}_{N_U})$. The energy harvested by the maritime user node is proportional to the noise-free part of the signal in (1), given by

$$\begin{aligned} E_U &= \eta\alpha T \mathrm{tr}\left(\mathbf{G}^H \mathbf{F}_R \mathbf{F}_R^H \mathbf{G}\right) \\ &= \eta\alpha T \mathrm{tr}\left(\frac{P_R}{N_R}\mathbf{G}^H\mathbf{G}\right), \end{aligned} \tag{2}$$

where $\mathrm{tr}\,(\cdot)$ denotes the matrix trace, and $\eta\,(0 < \eta < 1)$ is the energy conversion efficiency.

In the second time period, the maritime user node transmits the information signal vector $\mathbf{x} = \left[\sqrt{\frac{E_U}{N_U}}x_1, \sqrt{\frac{E_U}{N_U}}x_2, \ldots, \sqrt{\frac{E_U}{N_U}}x_{N_U}\right]^T$ to the aerial relay node with $\mathbb{E}\{\mathbf{x}\mathbf{x}^H\} = \sqrt{\frac{E_U}{N_U}}\mathbf{I}_{N_U}$. The received signal vector at the aerial relay node can be expressed as

$$\mathbf{y}_R = \mathbf{G}\mathbf{x} + \mathbf{n}_R\,, \tag{3}$$

where $\mathbf{n}_R$ is the zero-mean AWGN at the aerial relay node with $\mathbf{n}_R \sim \mathcal{CN}(\mathbf{0}, \sigma_{N_R}^2\mathbf{I}_{N_R})$ [18]. The signal-to-noise ratio (SNR) at the aerial relay node can be calculated as

$$\mathrm{SNR}_R = \frac{\mathbf{G}\mathbf{x}\mathbf{x}^H\mathbf{G}^H}{\sigma_{N_R}^2\mathbf{I}_{N_R}}\,. \tag{4}$$

Based on (4), the instantaneous rate at the aerial relay node can be expressed as [19]

$$\begin{aligned} \mathrm{R}_R &= \frac{1-\alpha}{2}T\log_2\left|\mathbf{I}_{N_R} + \mathrm{SNR}_R\right| \\ &= \frac{1-\alpha}{2}T\log_2\left|\mathbf{I}_{N_R} + \frac{\mathbf{G}\mathbf{x}\mathbf{x}^H\mathbf{G}^H}{\sigma_{N_R}^2\mathbf{I}_{N_R}}\right|, \end{aligned} \tag{5}$$

where $|\cdot|$ denotes the determinant of the matrix.

In the third time period, the $N_R \times N_R$ matrix $\mathbf{F}$ used by the aerial relay node pre-encodes the received signal and forwards it to the land source node. The signal vector received by the land source node can be represented as

$$\begin{aligned} \mathbf{y}_S &= \mathbf{H}\mathbf{F}\mathbf{y}_R + \mathbf{n}_S \\ &= \mathbf{H}\mathbf{F}\mathbf{G}\mathbf{x} + \mathbf{H}\mathbf{F}\mathbf{n}_R + \mathbf{n}_S, \end{aligned} \tag{6}$$

where $\mathbf{H} \in \mathbb{C}^{N_S \times N_R}$ represents the MIMO channel matrix between the aerial relay node and the land source node [20], $\mathbf{n}_S$ is the zero-mean additive white Gaussian noise at the maritime user node with $\mathbf{n}_S \sim \mathcal{CN}(\mathbf{0}, \sigma_{N_S}^2\mathbf{I}_{N_S})$ [21].

According to the Zero-Forcing/Zero-Transmission (ZFR/ZFT) techniques, the aerial relay node processes the received signal using ZF techniques and amplifies the transmitted signal using ZF transmission techniques. The ZFR/ZFT encoding matrix can be expressed as $\mathbf{F}_{zf} = \beta_{zf}\overline{\mathbf{F}_{zf}}$, where β_{zf} is the amplification factor of the ZFR/ZFT relay encoding matrix, $\overline{\mathbf{F}_{zf}}$ can be expressed as

$$\overline{\mathbf{F}_{zf}} = \mathbf{H}^H\left(\mathbf{H}\mathbf{H}^H\right)^{-1}\mathbf{A}\left(\mathbf{G}^H\mathbf{G}\right)^{-1}\mathbf{G}^H\,. \tag{7}$$

According to the power constraints of relay nodes $\mathrm{tr}\left[\mathbb{E}\{\mathbf{x}_R\mathbf{x}_R^H\}\right] = P_R$, where $\mathbf{x}_R = \mathbf{F}\mathbf{G}\mathbf{x} + \mathbf{F}\mathbf{n}_R$, can be obtained

$$\beta_{zf}^2 \left(\frac{E_U}{N_U} \mathrm{tr}\left(\overline{\mathbf{F}_{zf}} \mathbf{G}\mathbf{G}^H \overline{\mathbf{F}_{zf}}^H \right) + \mathrm{tr}\left(\overline{\mathbf{F}_{zf}\mathbf{F}_{zf}}^H \right) \right) = P_R \,. \tag{8}$$

According to (8), the amplification factor of the ZFR/ZFT relay encoding matrix can be expressed as

$$\beta_{zf} = \sqrt{\frac{P_R}{\left(\frac{E_U}{N_U} \mathrm{tr}\left(\overline{\mathbf{F}_{zf}} \mathbf{G}\mathbf{G}^H \overline{\mathbf{F}_{zf}}^H \right) + \mathrm{tr}\left(\overline{\mathbf{F}_{zf}\mathbf{F}_{zf}}^H \right) \right)}} \,. \tag{9}$$

From this, we can calculate the signal vector received by the land source node after processing by the ZFR/ZFT technique as

$$\begin{aligned} \mathbf{y}_S &= \beta_{zf}\mathbf{H}\mathbf{H}^H \left(\mathbf{H}\mathbf{H}^H\right)^{-1} \mathbf{A} \left(\mathbf{G}^H\mathbf{G}\right)^{-1} \mathbf{G}^H\mathbf{G}\mathbf{x} \\ &\quad + \beta_{zf}\mathbf{H}\mathbf{H}^H \left(\mathbf{H}\mathbf{H}^H\right)^{-1} \mathbf{A} \left(\mathbf{G}^H\mathbf{G}\right)^{-1} \mathbf{G}^H\mathbf{n}_R + \mathbf{n}_S \\ &= \beta_{zf}\mathbf{A}\mathbf{x} + \beta_{zf}\mathbf{A} \left(\mathbf{G}^H\mathbf{G}\right)^{-1} \mathbf{G}^H\mathbf{n}_R + \mathbf{n}_S. \end{aligned} \tag{10}$$

The SNR at the land source node can be expressed as

$$\mathrm{SNR}_S = \frac{\beta_{zf}^2 \mathbf{A}\mathbf{x}\mathbf{x}^H\mathbf{A}^H}{\beta_{zf}^2\sigma_{N_R}^2 \mathbf{A}(\mathbf{G}^H\mathbf{G})^{-1}\mathbf{A}^H + \sigma_{N_S}^2\mathbf{I}_{N_S}} \,. \tag{11}$$

According to (11), the instantaneous rate at the land source node can be expressed as

$$\begin{aligned} \mathrm{R}_S &= \frac{1-\alpha}{2} T \log_2 \left| \mathbf{I}_{N_S} + \mathrm{SNR}_S \right| \\ &= \frac{1-\alpha}{2} T \log_2 \left| \mathbf{I}_{N_S} + \frac{\beta_{zf}^2 \mathbf{A}\mathbf{x}\mathbf{x}^H\mathbf{A}^H}{\beta_{zf}^2\sigma_{N_R}^2 \mathbf{A}(\mathbf{G}^H\mathbf{G})^{-1}\mathbf{A}^H + \sigma_{N_S}^2\mathbf{I}_{N_S}} \right| . \end{aligned} \tag{12}$$

3 Simulations

In this section, we consider a scenario where there is no direct communication link between the land source node and the maritime user node, necessitating relay communication through the aerial relay node. The distances between the aerial relay node and the maritime user node, and between the aerial relay node and the land source node, are both 1 km. We assume that the MIMO channel matrix from the aerial relay node to the land source node and from the maritime user node to the aerial relay node are quasi-static, considering the open space above the sea with no obstructions, and due to the irregular wave motion of the sea surface and the evaporation waveguide produced above the sea surface by the evaporation of seawater, the direct and scattered paths of the signal coexist,

and the two channel matrices are modeled as $\mathbf{H} = D_{RS}^{\rho} L_{atmo}^{\tau} L_{sea}^{\xi} \widetilde{\mathbf{H}}_{Ric}$ and $\mathbf{G} = D_{UR}^{\rho} L_{atmo}^{\tau} L_{sea}^{\xi} \widetilde{\mathbf{G}}_{Ric}$, where ρ is the path loss exponent, τ is the evaporation waveguide attenuation index, and ξ is the sea surface reflection loss intensity, based on the communication environment above the ocean, we set the three parameters to $\rho = 2$, $\tau = 2$, and $\xi = 1$, respectively, $\widetilde{\mathbf{H}}_{Ric}$ and $\widetilde{\mathbf{G}}_{Ric}$ representing the Rician channel fading of the two channel matrices [22]. We assume that the equivalent noise power at the aerial relay node and the land source node is $\sigma_{N_R}^2 = \sigma_{N_S}^2 = -40\ dBm$. Unless specifically stated, we fix the time switching coefficient $\alpha = 0.5$, energy conversion efficiency $\eta = 0.8$, communication time $T = 1$ seconds, $N_U = N_S = N$.

Figure 2 depicts the relationship between the energy collected at the maritime user node and the energy power P_R transmitted by the aerial relay node with different numbers of antennas, where the number of antennas at the aerial relay node is fixed. It can be observed that the energy collected by the maritime user node increases with the increase of the transmission power P_R of the aerial relay node, and the energy collected also increases when the number of antennas N_U and N_S increases.

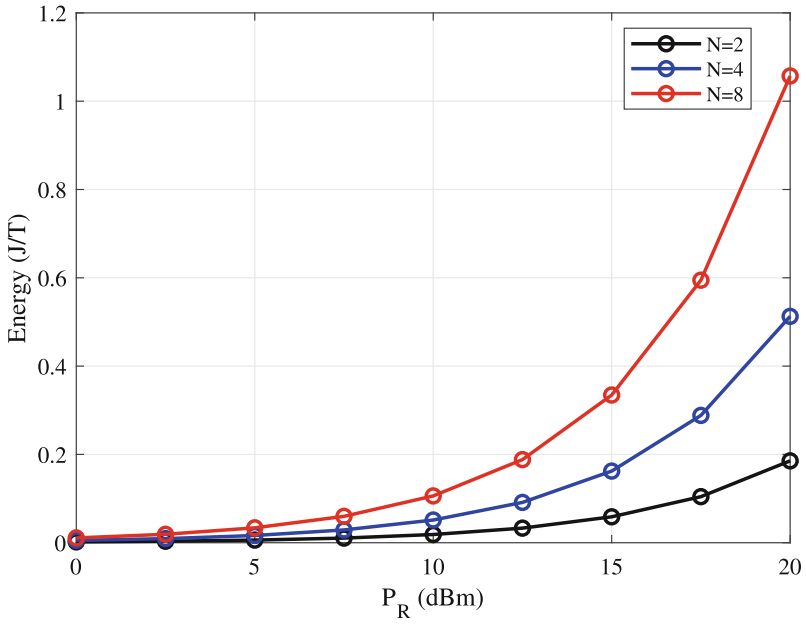

Fig. 2. Energy collection versus energy transmission P_R, $N_R = 8$.

Figure 3 shows that as the energy received by the maritime user node increases, the communication rate R_R from the maritime user node to the aerial relay node also increases, and the increase in the number of antennas N_U and N_S also leads to an increase in communication rate. Therefore, we can predict that

this will lead to an increase in the total communication rate from the maritime user node to the land source node.

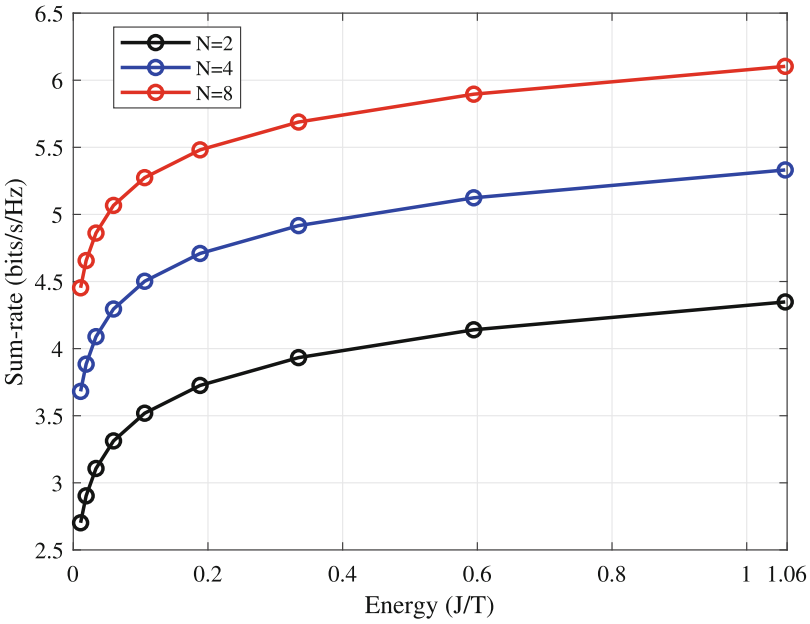

Fig. 3. R_R versus energy collection, $N_R = 8$.

Figure 4 confirms this, clearly showing that when the energy received by the maritime user node increases, there is a significant improvement in the communication rate R_S, and as the number of antennas increases, the communication rate R_S also increases.

To more clearly observe the impact of the number of antennas on communication performance, we analyzed the relationship between the achievable rates and the number of antennas N_R at the aerial relay node. Figures 5 and 6 shows the relationship between the achievable sum rate and the number of aerial relay nodes under different antenna configurations for maritime user nodes and land source nodes. It can be seen that whether it is the sum rate between the maritime user node and the aerial relay node, or the total communication rate from the maritime user node to the land source node, the system's rate performance is better when there are more antennas at the aerial relay node.

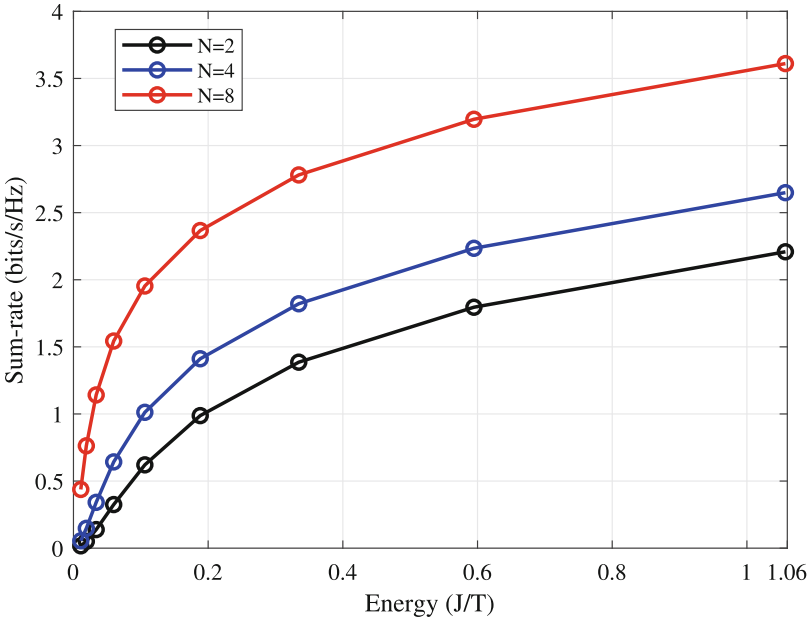

Fig. 4. R_S versus energy collection, $N_R = 8$.

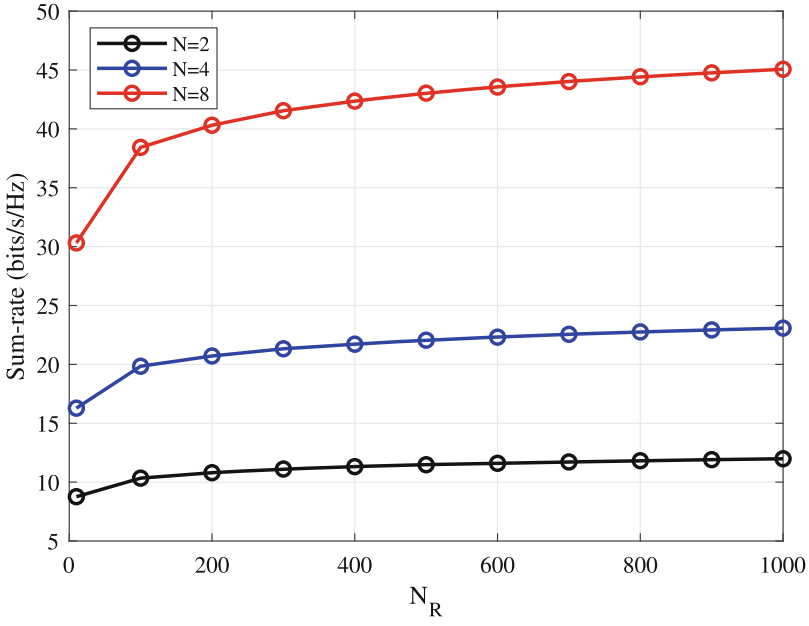

Fig. 5. R_R versus N_R.

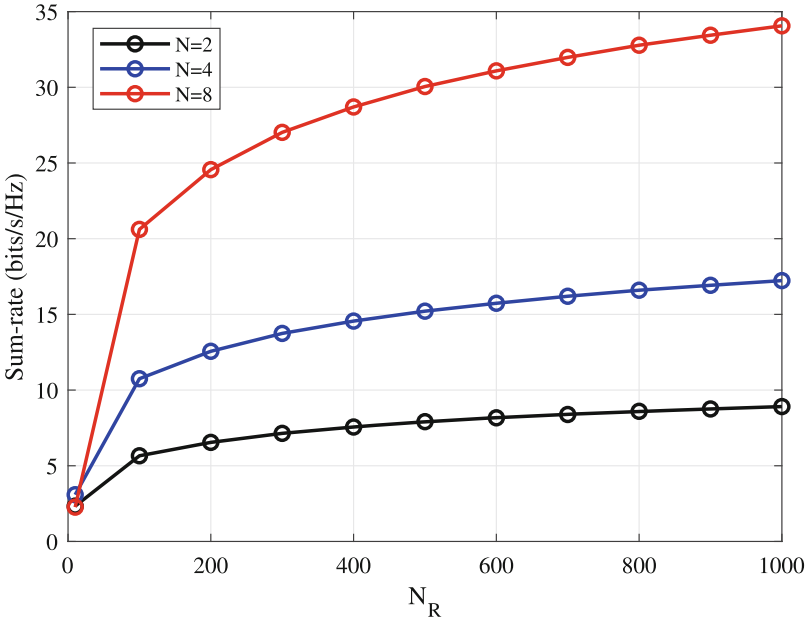

Fig. 6. R_S versus N_R.

4 Conclusion

In this paper, we propose a novel land-to-maritime user channel model. This model not only considers the need for maritime users without fixed power supply, such as buoys, to be wirelessly charged to start but also considers the unique points of maritime communication, such as the loss caused by evaporation ducts and reflections caused by sea surface fluctuations. On this basis, we derive and study the rate performance of a multi-antenna relay system in a marine communication environment.

References

1. Campos, R., Oliveira, T., Cruz, N., et al.: BLUECOM+: cost-effective broadband communications at remote ocean areas. In: OCEANS 2016, pp. 1–6. Shanghai, China (2016)
2. Kim, H, J., Choi, J, K., Yoo, D, S., et al.: Implementation of MariComm bridge for LTE-WLAN maritime heterogeneous relay network. In: 2015 17th International Conference on Advanced Communication Technology (ICACT), pp. 230–234. PyeongChang, Korea (South) (2015)
3. Mu, L., Kumar, R., Prinz, A.: An Integrated Wireless Communication Architecture for Maritime Sector. In: Sacchi, C., Bellalta, B., Vinel, A., Schlegel, C., Granelli, F., Zhang, Y. (eds.) Multiple Access Communications. MACOM 2011, Lecture Notes in Computer Science, vol 6886. Springer, Berlin, Heidelberg (2011)

4. Du, W., Ma, Z., Bai, Y., et al.: Integrated wireless networking architecture for maritime communications. In: 2010 11th ACIS International Conference on Software Engineering, Artificial Intelligence, Networking and Parallel/Distributed Computing, pp. 134–138. London, UK (2010)
5. Choi, M, S., Jeong, M, A., Jeon, S, M., et al.: Ship to shore maritime communication for e-Navigation using IEEE 802.16e. In: 013 International Conference on ICT Convergence (ICTC), pp. 759–762. Jeju (2013)
6. Manoufali, M., Alshaer, H., Kong, P, Y., et al.: Technologies and networks supporting maritime wireless mesh communications. In: 6th Joint IFIP Wireless and Mobile Networking Conference (WMNC), pp. 1–8. Dubai, United Arab Emirates (2013)
7. Cho, K., Kang, C, G., Yun, C: Transmission rate control of ASO-TDMA in multihop maritime communication network. In: 2012 International Conference on ICT Convergence (ICTC), pp. 85–86. Jeju, Korea (South) (2012)
8. Zhou, M, T., Hoang, V, D., Harada, H., et al.: high-speed maritime wireless mesh network. IEEE Wireless Commun. **20**(5), 134–142 (2013)
9. Qi, S., Lin, B., Dai, Y., Zhang, C., Hu, X.: Hypergraph-based modeling and throughput optimization for uav-assisted offshore communication networks. In:2023 IEEE 23rd International Conference on Communication Technology (ICCT), pp. 1153–1158. Wuxi, China (2023)
10. Duan, R., Wang, J., Zhang, H., et al.: Joint multicast beamforming and relay design for maritime communication systems. IEEE Trans. Green Commun. Network. **4**(1), 139–151 (2020)
11. Li, H., Yu, C., Zhang, C., Jiao, H., Lin, B., He, R.: Maritime multi-relay communications based on UAV trajectory adjustment and dual Q-learning. In: 2021 International Conference on Security. Pattern Analysis, and Cybernetics(SPAC), pp. 571–576. Chengdu, Chengdu (2021)
12. Ji, Y., Zhang, X., Zhang, G., et al.: Use of NOMA for maritime communication networks with P-DF relaying channel. China Commun. **17**(7), 236–246 (2020)
13. Zhang, Z., Pang, H., Georgiadis, A., et al.: Wireless power transfer-an overview. IEEE Trans. Industr. Electron. **66**(2), 1044–1058 (2019)
14. Feng, W., Tang, J., Yu, Y., et al.: UAV-enabled SWIPT in IoT networks for emergency communications. IEEE Wirel. Commun. **27**(5), 140–147 (2020)
15. He, X., Liu, S., Wu, J., et al.: Wireless power and information dual transfer system via magnetically coupled resonators. Commun. Eng. **3**(8)
16. Li, W., Yu, Q., Qiu, J.H., Qi, J.: Intelligent wireless power transfer via a 2-bit compact reconfigurable transmissive-metasurface-based router. Nature Commun. **15**(1) (2024). https://doi.org/10.1038/s41467-024-46984-4
17. Wang, W., Tang, J., Zhao, N., et al.: Joint precoding optimization for secure SWIPT in UAV-aided NOMA networks. IEEE Trans. Commun. **68**(8), 5028–5040 (2020)
18. Cheung, D.: The Air-Water Interface Stabilises Alpha-Helical Conformations of the Insulin B-Chain. ChemRxiv (2019)
19. Cao, X., Hu, X., Peng, M.: Joint mode selection and beamforming for IRS-aided maritime cooperative communication systems. IEEE Trans. Green Commun. Network. **7**(1), 57–69 (2023)
20. Li, J., Chen, M., Hou, S., Wang, Y., Luo, Q., Wang, C.: An improved S2A-Net algorithm for ship object detection in optical remote sensing images. Remote Sens. **15**(18), 4559 (2023)

21. Luo, Q., Shao, Y., Li, J., et al.: A multi-AUV cooperative navigation method based on the augmented adaptive embedded cubature Kalman filter algorithm. Neural Comput. Appl. **34**(21), 18975–18992 (2022)
22. Akhlaghpasand, H., Bjrnson, E., Razavizadeh, S, M.: Jamming-robust uplink transmission for spatially correlated massive MIMO systems. IEEE Trans. Commun. **68**6), 3495–3540 (2020)